Supporting information

Lipids	MIT	ER	NM	CM
DPPC (16:0/16:0)	**21.25**		**33.3**	**26.0**
POPC (16:0/18:1)		**18.75**		**20.7**
SAPC (18:0/20:4)	**20.0**			
YOPC (16:1/18:1)		**40.0**		
DOPC (18:1/18:1)			**22.7**	
DPPE (16:0/16:0)	**20.0**			
SAPE (18:0/20:4)	**20.0**			
DOPE (18:1/18:1)		**18.75**		
POPE (16:0/18:1)		**2.5**		
SOPE (18:0/18:1)			**7.3**	**10.0**
SLPE (18:0/18:2)			**4.0**	
PSM (18:1/16:0)		**2.5**	**14.0**	**13.3**
SOPS (18:0/18:1)		**1.25**	**2.0**	**12.0**
SAPI (18:0/20:4)	**2.52.1**	**10.0**	**2.010.0**	**1.3**
POPI (16:0/18:1)	**3.756**			**0.7**
PVCL2 (16:0,18:1/16:0,18:1)	**3.754.2**			
TLCL2 (18:2,18:2/18:2,18:2)	**5.07**			
POPA (16:0/18:1)		**1.25**	**0.7**	
		3		
DPPA (16:0/16:0)				**1.3**
Cholesterol	**3.754.2**	**5.03**	**14.75.3**	**14.7**

Table S1: Phospholipid composition for the different membrane models used in this study. MIT: outer mitochondrial, ER: endoplasmic reticulum, NM: normal plasma membrane and CM: cancer plasma membrane. Both the outer and inner layer of each bilayer membrane were built with the same lipid composition. In the first column abbreviations are used for the different phospholipids. The first value in the notation (#:#) indicates the number of carbons in the fatty acid chain and the second value the number of double bonds in the chain.

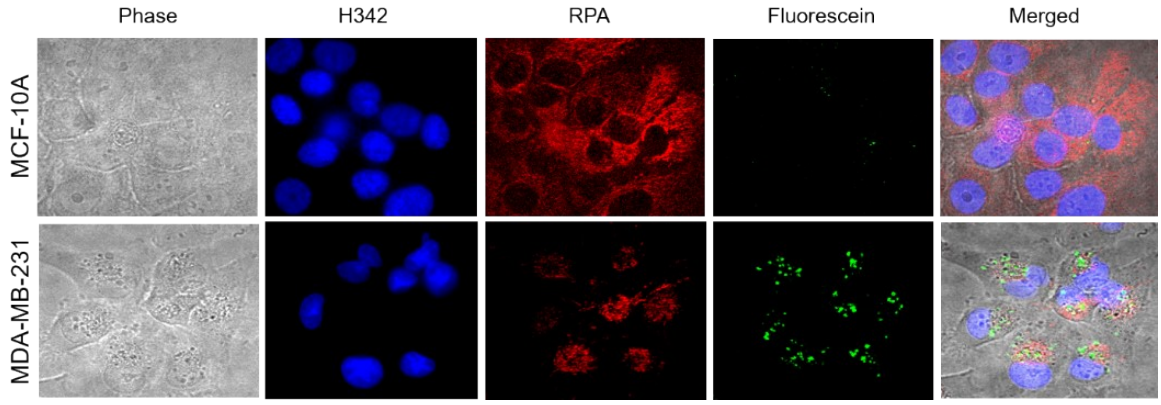

Figure S1: Preferential entry of the NAF-1^{44-67} peptide into malignant breast cancer cells. Representative semi-confocal images of MDA-MB-231 and MCF-10A cells stained with RPA (mitochondria) and Hoechst 342 (nuclei), in the presence of Fl- NAF-1^{44-67} peptide after 6h. The peptide penetrated mostly the MDA-MB-231 cells. The scale bar is 20 µm.

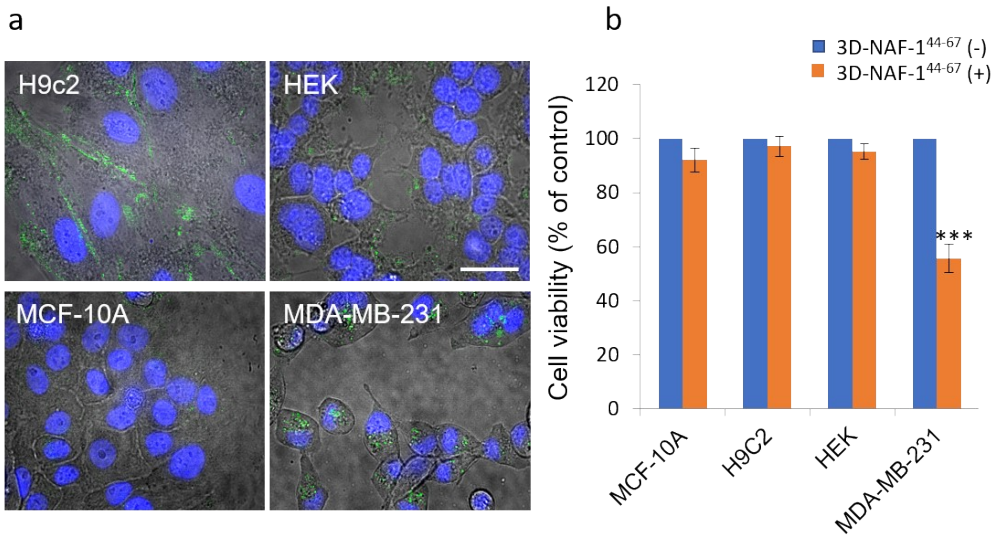

Figure S2: Entry of the 3D-NAF$^{44-67}$ peptide into malignant cells and its cytotoxicity toward different cell lines. Cells were incubated with FL-3D-NAF-1^{44-67} peptide for 3h and then washed with the medium. The nucleus was stained with Hoechst 33342. The fluorescence of fluorescein was monitored by semi-confocal microscopy. (a) Semi-confocal images of FL-3D-NAF$^{44-67}$ peptides in H9c2 (cardiac cells), HEK 293 (kidney cells), MCF-10A (normal breast cells) and in MDA-MB-231 (breast cancer cells). (b) Cytotoxicity of the 3D-NAF-1^{44-67} peptides in MCF-10A, H9c2, HEK 293 cells and in MDA-MB-231 cells was evaluated using Presto-Blue assay. The graph shows cell viability measurement for without 3D-NAF-1^{44-67} peptides (blue) and with 3D-NAF-1^{44-67} peptides (red) after 2 days of incubation. *** *P<0.001*. the scale bar is 50 µm.

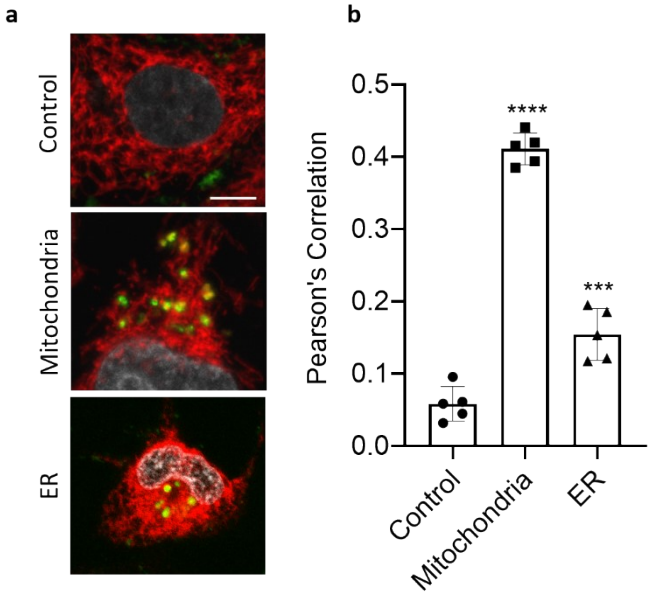

Figure S3: Colocalization of Fl-NAF-1$^{44-67}$ with the mitochondria and ER in cells. (a) Representative confocal images of MCF-10A (control) and MDA-MB-231 (mitochondria, ER) cells incubated with Fl-NAF-1$^{44-67}$. The images were taken after three hours of incubation with the peptide. Cells are stained with Rhodamine 800 (mitochondria), stably expressed with DsRed (ER) and Hoechst 342 (nuclei). The scale bar is 5 µm. (b) Pearson's correlation coefficient (PCCs) for the degree of colocalization between Fl-NAF-1$^{44-67}$ and mitochondria or ER using Volocity Software. Data is shown as mean ± SD of 35 cells from 5 different fields from 3 independent experiments. **** *P<0.0001*, *** *P<0.001* by t-test.

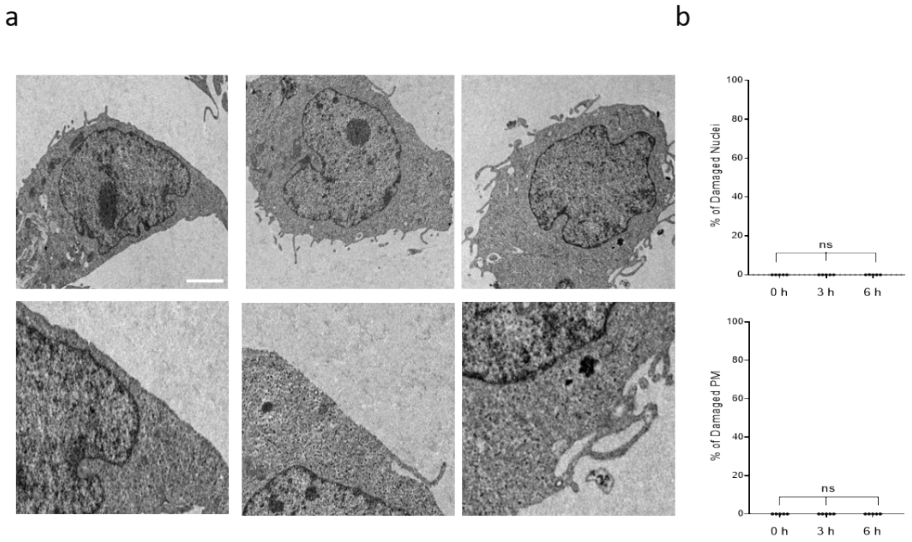

Figure S4: NAF-1$^{44-67}$ has a minimal effect on the PM and Nuclei of cancer cells. (a) Representative TEM images of Nuclei (top), PM (bottom) at different time points after incubation with 10 µM 3D-NAF-1$^{44-67}$. (b) Statistical analysis of changes in nuclei (top), PM (bottom) at different time points after incubation with 10µM 3D-NAF-1$^{44-67}$. NS denotes not

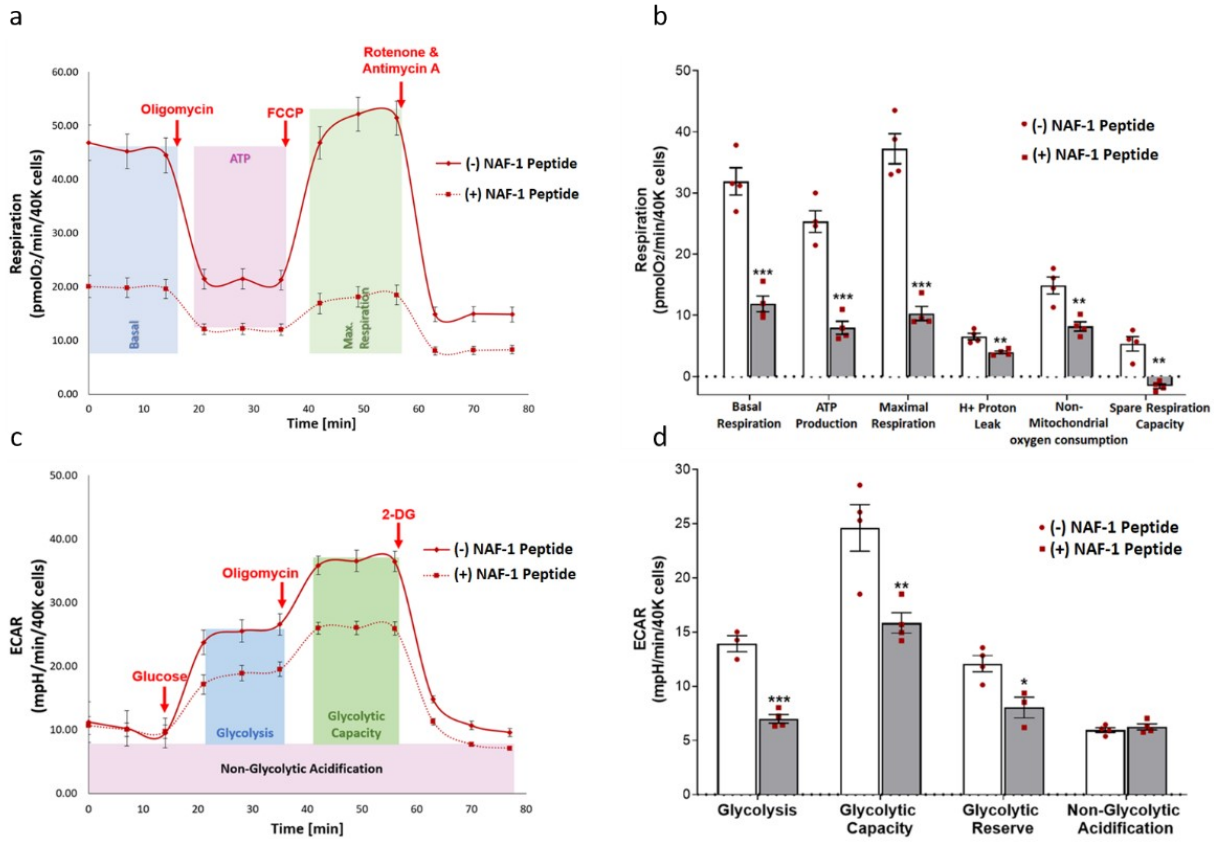

Figure S5: Seahorse measurements for oxygen consumption rate (OCR) and extracellular acidification rate (ECAR) of breast cancer MDA-MB-231 cells treated or untreated with the NAF-1$^{44\text{-}67}$ peptide. (a) OCR plots of mitochondrial respiration obtained for the different lines presenting the MDA-MB-231 cells control (continues line) compared to the NAF-1$^{44\text{-}67}$ peptide of 20μM (dot line). Data of OCR is presented in normalized values. (b) Different parameters calculated from the OCR experiment, summarizes the different mitochondria related activities for the cells with the NAF-1$^{44\text{-}67}$ peptide (gray columns) or without the NAF-1$^{44\text{-}67}$ peptide (white columns). Results presented as mean ± SD with all the data dots presented on the columns, student T-test was used to determine statistical significance of *P-value; *<0.5, **<0.01, ***<0.001*. (c) ECAR generated plots of cellular glycolysis ability obtained for the different lines presenting the MDA-MB-231 cells control (continues line) compared to the NAF-1$^{44\text{-}67}$ peptide of 20μM (dot line). Data of ECAR is presented in normalized values. (d) Different parameters calculated from the ECAR experiment, summarizes the different cellular glycolysis related activities for the cells with the NAF-1$^{44\text{-}67}$ peptide (gray columns) or without the NAF-1$^{44\text{-}67}$ peptide (white columns). Results presented as mean ± SD with all the data dots presented on the columns, student T-test was used to determine statistical significance of *P-value; *P<0.5, **P<0.01, ***P<0.001*. All data points measured in four different experiments. N=4.

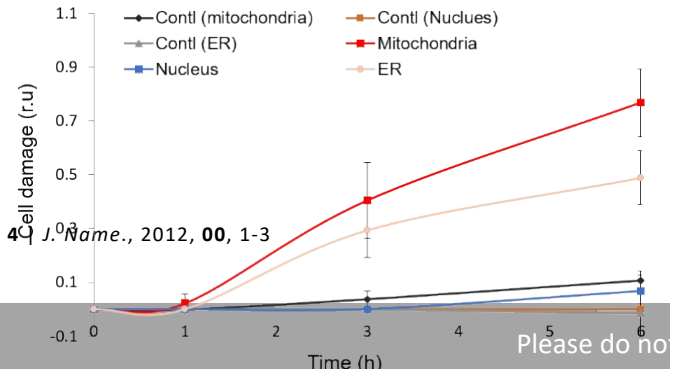

Figure S6: Time-course of peptide-induced intracellular structure damage in malignant epithelial breast cancer cells. Control MCF-10A and malignant MDA-MB-231 epithelial breast cells were pre-stained with Rhodamin 800 (mitochondria), DsRed (ER) and hoechst 33342 (nuclei) and incubated with the Fl- NAF-1$^{44\text{-}67}$ peptide (10 μM) for 0, 1, 3 and 6 hours. Damage to intracellular structures was quantified as described in Material and Methods using 75 cells from 15 different fields per time-point, from 3 independent experiments. *** denotes *P<0.001* by t-test.

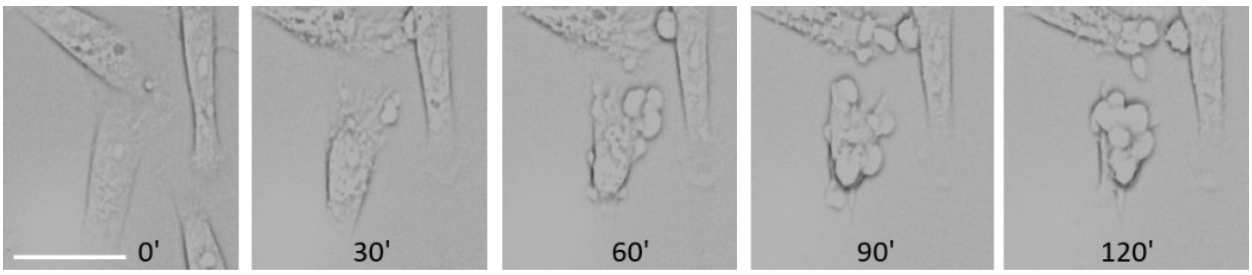

Figure S7: The peptide induces apoptotic bodies in MDA-MB-231 breast cancer cells. Cell phase images of apoptotic bodies at different time points in 3D-NAF-1$^{44-67}$ treated MDA-MB-231 cells. The scale bar is 30 µm.

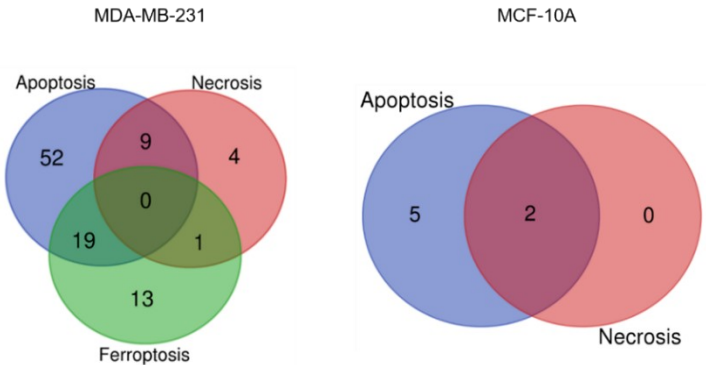

Figure S8: Venn diagrams generated from the proteomics analysis showing the correlation among the different cell death pathways in MDA-MB-231 cancer cells compared to MCF-10A normal cells.

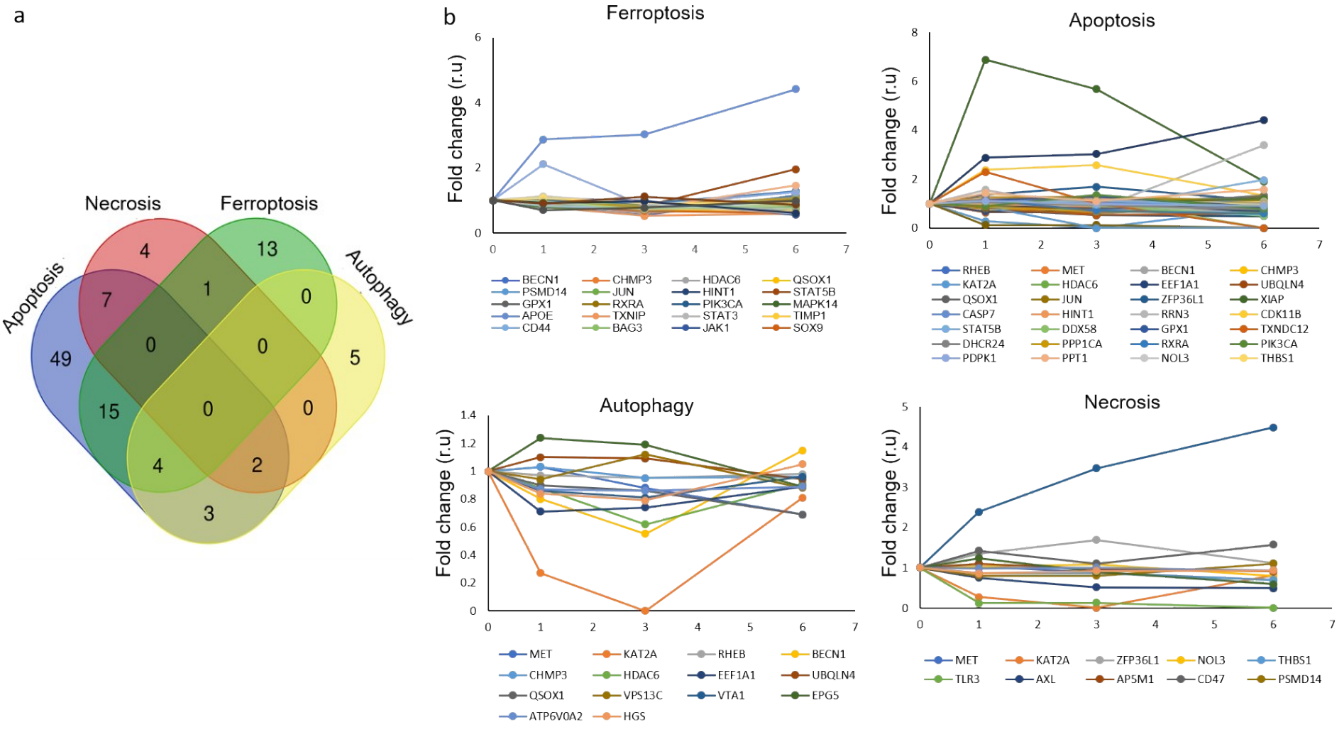

Figure S9: The NAF-1$^{44-67}$ peptide induces the expression of proteins associated with apoptosis, ferroptosis necrosis and autophagy in MDA-MB-231 cells. (a) Venn diagram generated from the proteomics analysis showing high occurrences of proteins related to apoptosis, ferroptosis, necrosis and autophagy and their correlation in MDA-MB-231 cells. (b) Time-course analysis of fold change in expression level of proteins associated with to apoptosis, ferroptosis, necrosis and autophagy.

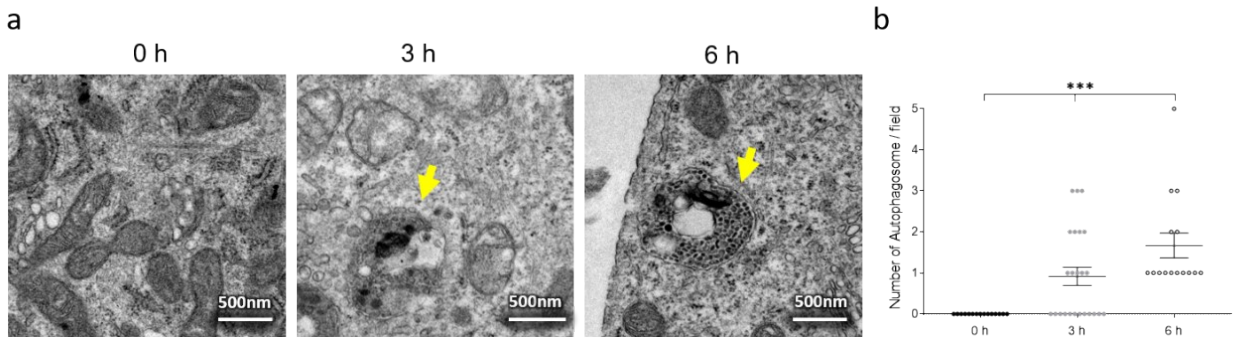

Figure S10: Peptide induced autophagy formation in TEM images. (a) Representative TEM images of autophagy at different time points after incubation with 10μM 3D-NAF-1$^{44-67}$. (b) Statistical analysis of changes in autophagy at different time points after incubation with 10μM 3D-NAF-1$^{44-67}$. ****P<0.001* by t-test.

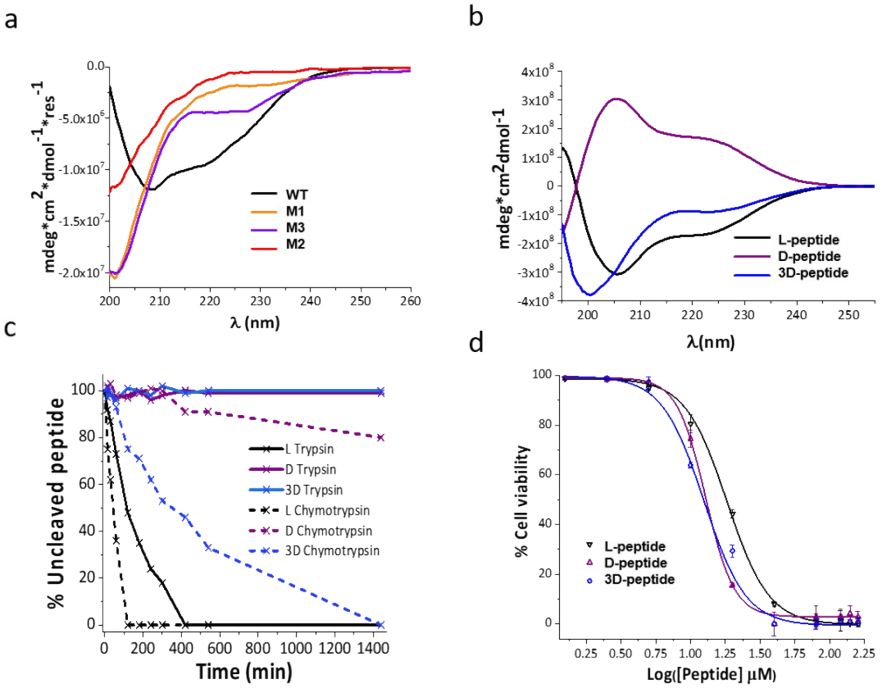

Figure S11: The full sequence of NAF-1$^{44-67}$ is required for its anti-cancer activity, and NAF-1$^{44-67}$ can be stabilized using D amino acids. (a) CD spectra of the NAF-1$^{44-67}$ fragments in 3 mM DPC. NAF-1$^{53-67}$ (orange) and NAF-1$^{57-67}$ (red), and NAF-1$^{44-52+62-67}$ (purple). (b) CD spectra of D-NAF-1$^{44-67}$ (purple) and 3D-NAF-1$^{44-67}$ (blue) compared to L-NAF-1$^{44-67}$ (black), all in 3 mM DPC. (c) Stability of the NAF-1$^{44-67}$ derived peptides in the presence of Trypsin (Solid line) or Chymotrypsin (Dash line). (d) IC50 value for inducing MDA-MB-231 cell death of peptides derived from NAF-1$^{44-67}$ (18.3 ± 0.4μM for L-NAF-1$^{44-67}$, 12.8 ± 0.2μM for D-NAF-1$^{44-67}$, and 12.5 ± 0.6μM for 3D-NAF-1$^{44-67}$).

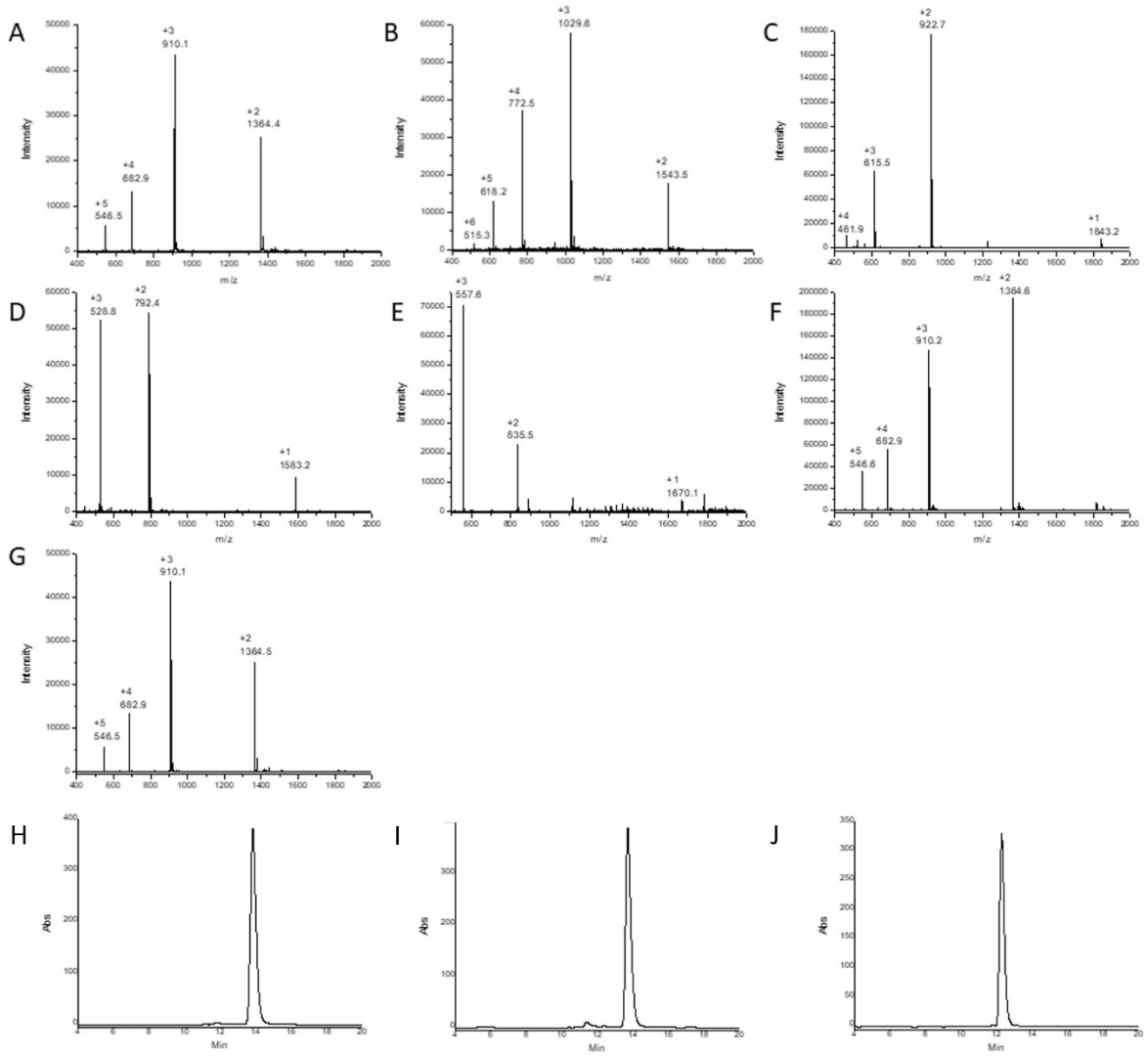

Figure S12: ESI-MS and analytical HPLC of peptides used in this research. (A) L-NAF-1 44-67. The calculated Mass is 2727.4 Da and the observed mass is 2727.1 Da; (B) FL-NAF-1 44-67. The calculated Mass is 3086.4 Da and the observed mass is 3085.7 Da; (C) NAF-1 53-67. The calculated Mass is 1843.3 Da and the observed mass is 1843.2 Da; (D) NAF-1 W57-67. The calculated Mass is 1582.9 Da and the observed mass is 1583.1 Da; (E) NAF-1 44-52+62-67. The calculated Mass is 1670.1 Da and the observed mass is 1669.6 Da; (F) D-NAF-1 44-67. The calculated Mass is 2727.4 Da and the observed mass is 2727.3 Da; (G) 3D-NAF-1 44-67. The calculated Mass is 2727.4 Da and the observed mass is 2727.1 Da; (H-J) Analytical HPLC analysis of (H) L-NAF-1 44-67, (I) D-NAF-1 44-67, (J) 3D-NAF-1 44-67.

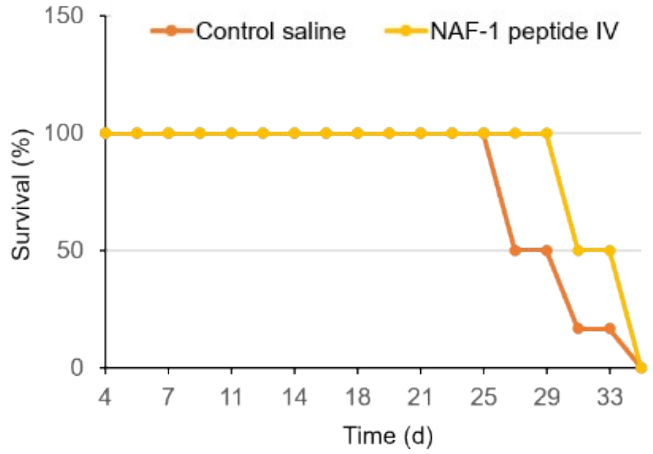

Figure S13: Mice survival curve demonstrating prolonged mice survival following treatment with the NAF-1$^{44-67}$ peptide *vs.* control.